HHS Public Access

Author manuscript

J Immunol. Author manuscript; available in PMC 2021 November 15.

Published in final edited form as:

J Immunol. 2021 May 15; 206(10): 2277–2289. doi:10.4049/jimmunol.2001211.

MYO1F regulates IgE and MRGPRX2-dependent mast cell exocytosis

Arnau Navinés-Ferrer[*,†], **Erola Ainsua-Enrich**[*,†], **Eva Serrano-Candelas**[*,†], **Elizabeth Proaño-Pérez**[*,†], **Rosa Muñoz-Cano**[†,‡,‖], **Gabriel Gastaminza**[§,‖], **Ana Olivera**[¶], **Margarita Martin**[*,†,‖]

[*]Biochemistry Unit, Biomedicine Department. Faculty of Medicine, University of Barcelona. Barcelona, Spain

[†] Laboratory of Clinic and Experimental Respiratory Immunoallergy (IRCE), IDIBAPS. Barcelona, Spain

[‡] Allergy Section, Pneumology Department, Hospital Clinic, University of Barcelona, Barcelona, Spain

[§] Department of Allergy and Clinical Immunology, Clínica Universidad de Navarra, Pamplona, Spain

[¶] Mast Cell Biology Section, Laboratory of Allergic Diseases, National Institute of Allergy and Infectious Diseases, National Institutes of Health, Bethesda, Md

[‖] ARADyAL research network

Abstract

The activation and degranulation of mast cells is critical in the pathogenesis of allergic inflammation and modulation of inflammation. Recently, we demonstrated that the unconventional long-tailed myosin, MYO1F, localizes with cortical F-actin and mediates adhesion and migration of mast cells. Herein, we show that knockdown of MYO1F by shRNA reduces human mast cell degranulation induced by both IgE-crosslinking and by stimulation of the Mas-Related G Protein-coupled Receptor X2 (MRGPRX2), which has been associated with allergic and pseudoallergic drug reactions respectively. Defective degranulation was accompanied by a reduced reassembly of the cortical actin ring after activation, but reversed by inhibition of actin polymerization. Our data shows that MYO1F is required for full Cdc42 GTPase activation, a critical step in exocytosis. Furthermore, MYO1F knockdown resulted in less granule localization in the cell membrane and fewer fissioned mitochondria along with deficient mitochondria translocation to exocytic sites. Consistent with that, AKT and DRP1 phosphorylation are diminished in MYO1F knockdown cells. Altogether, our data point to MYO1F as an important regulator of mast cell degranulation by contributing to the dynamics of the cortical actin ring and the distribution of both the secretory granules and mitochondria.

CORRESPONDENCE: M. Martin, Biochemistry Unit, Biomedicine Department. Faculty of Medicine, University of Barcelona, Carrer de Casanova 143, E-08036 Barcelona, Spain. martin_andorra@ub.edu. Phone: (34) 93-4024541. Fax: (34) 93-4035882.

INTRODUCTION

Human mast cells perform a variety of biological activities that are closely linked to their ability to release and secrete several mediators like histamine, leukotrienes, prostaglandins (1) and different cytokines. These mediators are important in host defense, innate and acquired immunity and homeostasis. Mast cell activation can induce the immediate release of preformed mediators present in secretory granules but also the synthesis and secretion of *de novo* mediators. Depending upon the stimuli involved, these events can be discriminated in a chronological manner and can involve different mediators and secretory pathways. The best studied mechanism is IgE-mediated degranulation which is mediated via the high affinity receptor for IgE (FcεRI). Crosslinking of receptor-bound IgE by a specific antigen results in the activation of different signaling pathways that promote the degranulation event (2). Various inflammatory products, such as cytokines, chemokines, and sphingosine-1-phosphate (S1P) (3) can also induce mast cell activation and they are important in the pathophysiology of various inflammatory conditions. Mast cells can recognize invasive pathogens through complement and pattern recognition receptor (PRR)-dependent pathways (4). They can also be triggered by neuropeptides such as corticotrophin-releasing hormone (CRH), neurotrophins and substance P (SP). The Mas-related G protein-coupled receptor X2 (MRGPRX2), is activated by substance P (5), and several drugs such as neuromuscular relaxants, opioids and vancomycin (6, 7).

Mast cell degranulation is a highly regulated process that relies on close interaction with receptors and signaling proteins, as well as fine regulation of the microtubule and actin cytoskeleton (8). On the one hand, the movement of secretory granules depends on intact microtubules, (9) which are stably anchored in the centrosome and grow from the center of the cell to the periphery. On the other hand, microfilaments, also called actin filaments, mostly concentrate just beneath the plasma membrane forming the cortical actin cytoskeleton. Actin filaments are involved in cell movement, changes in cell shape and organization of cytoplasmic components (10).

Recently, our group described the role of a long-tailed unconventional type I myosin called Myosin 1f (MYO1F) as a modulator of mast cell adhesion through the adaptor protein SH3-binding protein 2 (3BP2) (11, 12). The interaction between these two proteins was modulated by stem-cell factor (SCF), the ligand of the KIT receptor, and MYO1F silencing led to downregulation of β1 and β7 integrins on the mast cell membrane. In the same article, we also described the role of 3BP2 in mast cell migration, as this molecule has already been reported to have a role in mast cell survival via KIT (13) and mast cell degranulation via FcεRI (14). This unconventional myosin contains a pleckstrin domain (PH) that allows the localization to the plasma membrane through phosphorylated phosphatidyl-inositols (PIP3), the usual motor domain with an ATP-binding site, and a calmodulin-binding site. Furthermore, the presence of a SH3 protein-binding domain in the C-terminal region of MYO1F as well as MYO1E differentiates them from short-tailed myosins, and mediates the interaction between MYO1F and the adaptor protein 3BP2 (11). The role of MYO1F in mast cell degranulation, however, remains unknown.

MYO1F was initially described as a modulator of cell adhesion and motility in neutrophils through the augmentation of exocytosis of β2 integrin-containing granules (15). A recent study argued that in fact, the migration and extravasation defect in MYO1F KO neutrophils was due to its role in regulating squeezing and dynamic deformation of the nucleus during migration through physical barriers (16). In macrophages, MYO1F regulates M1-polarization by stimulating intercellular adhesion through integrin-αVβ3 (17). Along with MYO1E, MYO1F regulates adhesion turnover during phagocytosis, creating membrane-cytoskeleton crosstalk through Fc-receptors that is indispensable for correct phagocytosis (18).

In this study, we describe the role of MYO1F in regulating IgE-dependent and - independent degranulation through MRGPRX2 and the involvement of the actin cytoskeleton in these processes. We also describe MYO1F as a key regulator of mitochondrial movement and fission after mast cell activation. Altogether, these results shed some light on the involvement of long-tailed, unconventional myosins in the dynamic events that are crucial for mast cell function and pathophysiology.

MATERIALS AND METHODS

Cell lines and reagents

The LAD2 human mast cell line kindly provided by Drs. A. Kirshenbaum and D.D. Metcalfe (National Institutes of Health, Bethesda, MD) was grown in StemPro-34 media (Life Technologies, Carlsbad, CA), supplemented with StemPro-34 nutrient and L-glutamine (2mM), penicillin (100 U/mL) and streptomycin (100 μg/mL), and 100 ng/mL SCF (Amgen, Thousand Oaks, CA) (19). Primary human mast cells (huMCs) derived from CD34-positive peripheral blood cells were obtained from healthy donors following informed consent using a protocol (98-I-0027) approved by the NIAID IRB, and differentiated *in vitro* for 8 weeks in the presence of 100 ng/ml IL-6 and 100 ng/ml SCF as previously described (20). After 8 weeks, culture purity was assessed by surface FcεRI and KIT expression. The HEK 293LTV cell line (Cell Biolabs Inc, San Diego, CA, USA) was used for lentivirus production.

Antibodies and other reagents

Mouse antibodies, α-MYO1F C5, α-KIT (clone Ab81), α-DRP1 C5, α-pAKT (Ser 473) were purchased from Santa Cruz (Santa Cruz Biotechnology, Inc. Santa Cruz, CA, USA). α-pDRP1 (Ser616) and α-pERK (Thr202/Tyr204) were from Cell Signaling (Cell Signaling Technology, Denvers, MA. Mouse α- Cdc42 from Cytoskeleton (Cytoskeleton Inc., Denver, CO). Goat α-mouse alexa-647 and goat α-rabbit alexa-488 were from Life Technologies (Carlsbad, CA), mouse α-human- Fc RI-PE from eBioscience (San Diego, CA). PE anti-human MRPGRX2 clone K125H4 was from Biolegend (Biolegend, San Diego, CA). TOM20 rabbit polyclonal Ab was from Proteintech (Rosemont, IL) and mouse monoclonal CD63-APC (clone MEM-259) was from Immunotools GmbH (Friesoythe, Germany).

Biotinylated human IgE (IgEB) was obtained from Abbiotec (San Diego, CA). Anti- mouse-HRP Ab was obtained from DAKO (Carpinteria, CA). Streptavidin, puromycin, doxycycline

hyclate, mouse α-tubulin (DM1A) and anti-β-actin (clone AC-40) were purchased from Sigma (Sigma- Aldrich, St. Louis, MO). Substance P was from AnaSpec (Fremont, CA).

Lentiviral transduction

Lentiviral particles were generated according to the manufacturer's instructions (Sigma-Aldrich, St. Louis, MO) as described elsewhere (11). We used two constructs for Myo1f knockdown: the lentiviral plasmid used in huMCs, with the shRNA sequence for MYO1F silencing, was from Origene Technologies (sequence D).

For LAD2, we used the TRCN0000158118 shRNA sequence (which partly overlaps with sequence D), CGTCTTCAAGACCGAGTTTGT, cloned into a doxycycline inducible lentiviral Tet-pLKO-puro plasmid (Addgene plasmid 21915) (21). Knockdown of MYO1F in cells was induced by adding 0.5 μg/mL doxycycline.

Degranulation Assays

For IgE-dependent activation we pre-incubated cells with or without IgEB (0.1 μg/ml) overnight in culture media without SCF. Cells were stimulated at 37°C with streptavidin (10–1000 ng/ml) to induce IgE crosslinking, with substance P (SP, 0.05–5μM) or with ionomycin (200 μg/mL) + PMA (10 ng/mL). Degranulation was analyzed based on the levels of β-hexosaminidase activity at the supernatant or on CD63 expression on the cell membrane, assessed by flow cytometry, as described in previous studies (7). To inhibit actin polymerization cells were pre-incubated with Latrunculin B (1μM) or Cytochalasin D (2μM) for 20 minutes before stimulation.

Imaging flow cytometry assay

Cells were activated or inhibited as described above. Afterwards, cells were fixed in PFA 4% - phosphate buffered saline (PBS) at 4oC. Cells were permeabilized with Saponin buffer (PBS-0.05% Saponin) for 15 minutes, blocked with blocking buffer (0.2% skimmed milk, 22% FCS, 1% bovine serum albumin (BSA), 0.01% triton X-100, 0.01% NaN3, dissolved in PBS) for 1 at 4oC. We used primary antibodies (TOM20 or CD63) (0.1–0.2 μg/100.000 cell) for 2 h of incubation at 4oC. At last, we used goat anti- rabbit or goat anti-mouse secondary antibodies labeled with Alexa-488 or Alexa-647 respectively for 45 minutes (dilution 1:300 – 1:500) at 4oC. For actin staining we used phalloidin-TRITC (dilution 1:500 – 1:1000).

Preparations were visualized and analyzed with an Amnis ImageStream® (Luminex®). All images were processed with AMNIS IDEAS® software. Cytoplasmic area vs. membrane area were determined with a mask and the cells were divided in: cells with fluorescence associated to plasma membrane or cells with fluorescence on the cytoplasm. Then, we quantified the percentage of cells showing localization mostly near the cell membrane in control (non-target shRNA) or MYO1F shRNA mast cells before or after stimulation.

Immunoblotting

Cells were sensitized overnight with biotinylated IgE (100 ng/ml) in culture media. The following day, the cells were stimulated at 37 °C with 400 ng/ml SA to induce IgE crosslinking, alternatively cells were treated with 2 μM of substance P in Tyrode's buffer for

the indicated times. Whole-cell lysate were solubilized in RIPA lysis buffer (1% Triton X-100, 5mM EDTA, 0.5% sodium deoxycholate, 0.1% SDS, 50 mM Tris [pH 7.4], 150 mM NaCl, 100 mM NaF, 1 mM Na_3VO). Total cell lysates were separated by SDS-PAGE and electrotransferred to polyvinylidene difluoride membranes (Millipore, Bedford, MA). Blots were probed with the indicated Abs. In all blots, proteins were visualized by ECL (Santa Cruz Biotechnology).

FACS staining

FcεRI and MRGPRX2 expression was detected by direct staining with the indicated Abs for 30 minutes at 4°C. KIT expression was detected using the primary antibody plus a secondary goat anti-mouse antibody with Alexa-647. Cells were analyzed using a FACSCalibur flow cytometer (FACScan; BD Biosciences). In all cases dead cells were excluded based on their Forward (FSC) and side scattering (SSC) profile.

Calcium release and mitochondrial membrane potential determination (TMRM)

Cells were pre-incubated for activation as described above and then washed and incubated with Fluo-4, AM (Invitrogen) or TMRM (ThermoFisher Scientific) for 20 minutes prior cell activation with IgEB plus streptavidin, SP or just ionomycin. Fluorescence was determined using a TECAN SPARK microplate reader.

PGD2 release and TNFα secretion assay.

PGD2 and TNFα release were determined from the supernatants of cells activated for 4 h or 24 h respectively using a specific EIA for PGD2 (Cayman Chemical) and a specific ELISA for TNFα (R&D systems) according to manufacturer's instructions.

Active GTPase Assays

GTPase activation assay was performed using Cdc42 G-LISA kits following manufacturer's instructions (Cytoskeleton) as well as described elsewhere (22). Briefly, Cell lysates ($1,5 \times 10^5$ cells x triplicate) were prepared using G-LISA lysis buffer, snap-frozen in liquid nitrogen and processed within 2 weeks after preparation. Lysate aliquots, corresponding to Cdc42 assay, were applied, respectively, to wells coated with Cdc42-GTP-binding protein. Active, GTP-bound GTPases bound to the wells were detected with the corresponding specific Ab. Constitutively active proteins were used as a standard.

Transmission electronic microscopy (TEM)

LAD2 mast cells, previously incubated with IgEB were activated with streptavidin (200 ng/mL) for 30 minutes, washed with PBS and pelleted. The pellet was fixed in 2.5% PFA and 2.5% glutaraldehyde in phosphate buffer 0.1M. After that, samples were processed for TEM and images were taken with a Jeol JEM 1010 100kv TEM microscope.

Data analysis

All results are expressed as mean ± standard error of the mean (SEM). Unpaired student ´s t-test or one-way ANOVA were used to determine significant differences (p- value) between

two or several experimental groups, respectively, after determination of normal distribution of the sample and variance analysis.

RESULTS

MYO1F is critical for IgE-dependent mast cell degranulation

The doxycycline-inducible MYO1F shRNA already described elsewhere (11) was used to determine the effect of MYO1F downregulation on mast cell degranulation, with non-target shRNA as a control. MYO1F protein knockdown in LAD2 mast cells was confirmed by western blot (Figure 1A). We measured degranulation as β-hexosaminidase release after IgEB-crosslinking at different doses of streptavidin after 30 minutes in LAD2 mast cells (Figure 1B). MYO1F shRNA cells showed reduced degranulation compared to non-target shRNA cells in the doxycycline-induced group. To determine whether this effect was delayed, we analyzed mast cell degranulation at several time points using CD63 as a marker. CD63 is found in granule membranes and it is exposed to the plasma membrane during degranulation. As demonstrated by FACS analysis (Figure 1C), MYO1F shRNA cells were unable to achieve similar degranulation levels as non-target shRNA cells, even after 3 hours.

We extended the study to CD34-derived huMCs. For this purpose, CD34-derived huMCs were induced to differentiate with IL-3, IL-6 and SCF as described in Material and Methods section. Cells were transduced with a MYO1F shRNA plasmid or scrambled-shRNA (non-target shRNA) using lentivirus at week 7 of mast cell differentiation and transduced cells were selected with puromycin. Knockdown was confirmed by western blot and the levels of KIT and FcεRI were checked by flow cytometry (Figure 1D). Similar to LAD2 mast cells, we observed a decrease in the extent of degranulation in MYO1F shRNA cells compared to non-target shRNA cells after 30 minutes (Figure 1E).

MYO1F is also necessary for MRGPRX2 mast cell degranulation

MRGPRX2 (Mas-related G protein-coupled receptor X2) has emerged in recent years as an important receptor in pseudoallergic drug reactions and has been implicated in innate and adaptive responses (23). Degranulation induced by MRGPRX2 and other GPCRs is a rapid piecemeal process that, unlike degranulation induced by IgE and IgG-receptors, does not involve granule fusion before exocytosis. We used substance P (SP) to activate MRGPRX2. Similar to the results shown in Figure 1, we observed that mast cell degranulation was impaired in MYO1F shRNA cells at several doses (Figure 2A). In addition, CD63 release from MYO1F-silenced cells was lower at all assessed times (Figure 2B). In CD34-derived huMCs, MRGPRX2 expression was similar in non-target shRNA cells and MYO1F shRNA cells (Figure 2C) however substance P-induced degranulation was significantly lower in MYO1F knockdown cells (Figure 2D).

TNF secretion but not PGD2 release is impaired in MYO1F-knockdown cells

Apart from the release of preformed pro-inflammatory mediators, activated mast cells can induce the early synthesis of prostaglandins and leukotrienes and subsequently the synthesis of cytokines like IL-4 and TNFα (24, 25). To examine whether MYO1F shRNA also affects the release of the *de novo* synthesized pro-inflammatory components we measured PGD2

release at 4h after IgE-crosslinking or substance P stimulation. PGD2 release, which is an example of transporter-mediated secretion, was similar in both groups (Supplementary Figure 1A). However, TNFα secretion, reported to occur by constitutive exocytosis (26), was diminished 24 h after substance P activation in MYO1F shRNA cells compared to non-target shRNA cells (Supplementary Figure 1B). Release of TNFα induced pharmacologically by Ionomycin plus PMA was not different in MYO1F shRNA cells, indicating that there was a defect in release rather than a different TNF content within the cells. These results show a differential role for MYO1F in regulating the exocytosis of preformed pro-inflammatory mediators and cytokines versus lipidic *de novo* pro-inflammatory mediators.

Myo1F is required for Cdc42 GTPases activation through FcεRI and MRGPRX2 in Mast Cells

Rho family GTPases play an important role in rearrangement of actin cytoskeleton (8, 27) and exocytosis (28). Specifically, it has been shown that GTPase Cdc42 regulates and coordinate vesicle transport with actin cytoskeletal rearrangements, events that trigger exocytosis (29, 30). Indeed, GTPase Cdc42 activation was maximal 2–5 minutes after MRGPRX2 activation in LAD2 cells (Figure 3A), while the activation pattern via FcεRI was slower, with maximal activation after 5–10 min (11). Thus, we examined the activation of small GTPases Cdc42 by IgEB-streptavidin (400 ng/mL) or substance P (2 μM) at the peak of activation in MYO1F-knockdown LAD2 mast cells. Our results showed that knockdown of MYO1F significantly reduced Cdc42 activity 5–10 minutes after IgEB-stv activation (Figure 3B), or 2–5 minutes after MRGPRX2 activation (Figure 3C) compared to non-target control cells. Although the basal levels of Cdc42 activity are also significantly reduced in Myo1f Knockdown cells, the total level of Cdc42 GTPase was not affected by MYO1F knockdown (Figure 3D). Taken together, our results suggest the involvement of MYO1F in the axis GTPases-actin rearrangement and exocytosis.

Inhibition of actin polymerization can restore the loss of degranulation of MYO1F knockdown mast cells

The phenotype observed during mast cell degranulation by IgE suggested that MYO1F cooperates with the actin cytoskeleton, specifically in the cortical actomyosin ring that is necessary for mast cell degranulation (31). It has been reported that mast cell degranulation is enhanced after inhibition of actin polymerization (32). Taking this into consideration, we measured degranulation after preincubating non-target shRNA and MYO1F-shRNA cells with the actin polymerization inhibitors Latrunculin B and Cytochalasin D. Mast cells were then stimulated by IgE crosslinking (Figure 4A) or substance P (Figure 4B). We observed that mast cell degranulation was enhanced using these inhibitors in control cells and that the degranulation capacity of MYO1F shRNA cells could be significantly recovered, although not up to the same levels as in control cells.

MYO1F knockdown reduces cortical actin rearrangement

Like all unconventional myosins, MYO1F colocalizes with the cortical actin ring in neutrophils and mast cells (11, 15). Mast cell activation by FcεRI causes degranulation in a process that involves the reorganization of the actin cytoskeleton. Pfeiffer et. al. first

reported that the actin content of mast cells during degranulation decreases during the first 10–30 s of antigen binding but then increases to almost double the control levels after 1 minute (33). These rearrangements are mediated by a plethora of proteins but seem to be critical for exocytosis (34). To determine the effect of MYO1F knockdown on the pattern of actin reorganization, we looked at the actin cytoskeleton by imaging flow cytometry after IgE-dependent activation of LAD2 mast cells for 15 minutes, using phalloidin-TRITC. As seen in Figure 5A, the cortical actin ring was clearly defined in control cells after IgE-dependent activation whereas in MYO1F shRNA cells the cortical actin ring was indistinct. Indeed, in those cells the actin ring was rearranged in clusters. The same phenotype was seen in CD34+-derived huMC where MYO1F was silenced (Figure 5B). Granule distribution in those cells was also determined using CD63 as a marker. After IgE-dependent stimulation granule translocation to the membrane could be observed by a shift in the CD63 fluorescence from the center of the cell (internal) to the periphery (external). As expected, MYO1F shRNA cells showed less external translocation than non-target shRNA cells (Figure 5C).

MYO1F silencing does not impair calcium signaling

Calcium mobilization in response to IgE crosslinking and MRGPRX2 is crucial for the degranulation process and there is a relationship between Ca2+ flux and exocytosis after mast cell stimulation (35). We therefore wanted to determine whether calcium signaling on MYO1F shRNA cells is affected. For this reason, we activated mast cells via IgE or with SP stimuli and determined the calcium signal using the fluorescent marker Fluo4. Our data shows that the calcium signal in non-target shRNA cells and MYO1F shRNA cells was similar (Supplementary Figure 2A). Elevations in cytosolic calcium after activation of mast cells occurs by release of calcium from intracellular stores and by store-operated Ca2+ entry (SOCE), which is activated in response to endoplasmic reticulum Ca2+ store depletion. To measure the contribution of calcium release from intracellular stores, we stimulated cells in the absence of calcium in the cell media. As shown in Supplementary Figure 2B, in the absence of extracellular calcium the calcium peaks were of lower magnitude than those in Supplementary Figure 2A. Under these conditions, we observed slight but significant differences in the calcium responses to IgE and SP in MYO1F- knockdown cells compared to non-target shRNA cells (right panels). These results indicate that intracellular calcium release is partly impaired by MYO1F knockdown, although the impairment is not sufficient to inhibit store-operated Ca2+ entry.

Mitochondrial fission and translocation to the cell membrane are altered in MYO1F knockdown mast cells after IgE-dependent activation

Mitochondria not only generate ATP but also regulate cellular calcium signals by accumulating and releasing Ca2+ (36). Mitochondria undergo fission into independent structures and translocation to the cell membrane after cell activation (37). Translocation may be necessary to provide energy locally or to maintain the calcium signal (37), while fission generates new organelles in stress conditions (38) and enhances mitochondrial mobility (39). Because mitochondria fission and translocation are important for degranulation and TNF production (37), we analyzed the shape of mitochondria using electron microscopy. As shown in Figure 6A, MYO1F-deficient cells showed more

elongated mitochondria after stimulation, indicating fewer fissioned mitochondria than in non-target cells. We also determined mitochondrial translocation after IgE-dependent degranulation using imaging flow cytometry, with TOM20 as a marker. In this case, the percentage of mitochondrial translocation in MYO1F-silenced cells was lower than that in control cells (Figure 6B).

Despite the differences in mitochondrial shape and translocation after activation in MYO1F knockdown cells, we did not observe any significant differences in mitochondrial membrane potential after IgE or substance P activation (Supplementary Figure 3), as determined using tetramethylrhodamine methyl ester (TMRM). Altogether, our data suggest that the mitochondrial morphology and localization during activation is, at least partly, regulated by MYO1F.

Myo1f knockdown regulates DRP1 phosphorylation leading to a block in mitochondrial fission

It is known that mitochondria can undergo fusion or fission depending on the dynamics of the cell (40, 41). During mast cell degranulation and cytokine secretion, the mitochondria will provide energy to perform these processes. The mitochondria will fission and translocate to the membrane to supply energy locally (42). As shown in Figure 7, MYO1F-deficient cells exhibited less mitochondrial fission compared to non-target cells. A key player in the fission process is a dynamin-related protein 1 (Drp1) a conserved dynamin member of a GTPase superfamily protein that facilitates membrane remodeling in a variety of cellular membranes (43, 44) and their phosphorylation on Ser616 is needed in order for mitochondrial division to occur (40, 45, 46). Thus, we explored the effect of DRP1 phosphorylation in MYO1F-silenced cells. Western blot analysis revealed that deficiency in MYO1F resulted in marked reductions in the phosphorylation of DRP1 after activation with either IgE^{B}-streptavidin (400 ng/mL) or substance P (2 μM). Effector pathways downstream of AKT and MAPK have also been reported to directly activate DRP1 and promote mitochondria fission (47). Thus, the levels of AKT and ERK phosphorylated were assessed. AKT phosphorylation, unlike ERK phosphorylation, was also markedly reduced in MYO1F-silenced cells (Figure 7). Taken together, our results suggest that MYO1F may play a role in mitochondria fission by regulating DRP1 phosphorylation.

DISCUSSION

The hallmark of the allergic reaction is the immediate release of inflammatory mediators located in the secretory granules of mast cells by regulated exocytosis. This event may occur by diverse mechanisms: full degranulation, kiss-and-run exocytosis, piecemeal degranulation, and compound exocytosis. All of these models occur in mast cells, although in vivo the predominant form is the compound exocytosis, mediated by IgE, in which several secretory granules merge together to form larger and heterogeneous secretory granules which then fuse with the plasma membrane (48). The mode of exocytosis also depends on the type of stimulus. Certain signals, including substance P, the complement anaphylotoxins C3a and C5a, and endothelin 1, induce human mast cells to rapidly secrete small and relatively spherical granule structures, a pattern consistent with the secretion of individual

granules (49). Thus, IgE-dependent mast cell activation produces patterns of degranulation that vary in spatiotemporal features and in the structural characteristics of the released granules from GPCR-dependent degranulation. Herein we show that in MYO1F-deficient cells, both types of exocytosis are impaired indicating a relevant role of this myosin in the release of preformed granules.

Apart from the immediate release of preformed mediators, mast cells also release lipid mediators that are de novo synthesized and released immediately from activated cells rather than stored. One example of that is prostaglandin D2 (PGD2), a mast cell specific eicosanoid, derived from arachidonic acid. PGD2 has bronchoconstricting and vasoactive properties and has an important role in host defense (50). Little is known about their secretion mechanism although it has been proposed that the mode of secretion is not only stimulus-dependent but also cell type dependent (48). It is known that eicosanoids are negatively charged at physiological pH and thus their secretion involves facilitated transport across the membrane through organic or anion transporters of the ATP-binding cassette type C family (51) or anion transporter solute carrier superfamily (52). Our results show that PGD2 is synthesized after IgE and MRGPRX2 activation and the reduction of MYO1F expression do not impair its secretion suggesting a selective action of MYO1F in the exocytic pathways of proinflammatory mediators. Among the large number of cytokines and chemokines released after cell activation, TNF is known to be pre-stored in mast cell granules (53), and can be released by regulated exocytosis, as well as synthesized following mast cell activation and released through constitutive exocytosis (26). Interestingly, in this case we found a dependence of MYO1F expression in TNF secretion. Altogether, we found that the role of MYO1F varies according to the specific type of secretion.

The Rho family GTPases play key roles in exocytotic processes and in actin polymerization (28, 54). It is known that Cdc42-WASP-Actin polymerization axis is important for degranulation and TNF secretion mediated by FcεRI activation (55). Our results adds to this pathway by involving MYO1F as a player in the regulation of active Cdc42 levels not only in cells stimulated via IgE/antigen but also via MRGPRX2 receptor activation, thus promoting degranulation and secretion of certain cytokines.

MYO1F, like all unconventional myosins, binds to cortical F-actin, (as demonstrated by colocalization studies in neutrophils and mast cells) (11, 15). The actin cytoskeleton is part of the secretory machinery. Actin has been proposed to serve as a barrier to exocytosis, preventing fusion of the secretory granules with the plasma membrane, but may also play a role in the trafficking of these granules and assisting in the expulsion of their contents outside of the cell (24). In unicellular models like *Dyctiostelium*, it has been shown that MYO1F is responsible for the inhibition of actin waves with dependence of its membrane binding site but not the motor site (56). This actin waves are seen in mast cells during IgE antigen-stimulation of FcεRI, driving a coordinated transformation of F-actin structures necessary for granule secretion (34). This process is a dynamic assembly and disassembly of cortical actin accompanied by changes in cell surface polarization (57). We demonstrated that cortical actin reorganization was impaired after IgE activation in MYO1F-knockdown cells, leading to a defective granule extrusion. Furthermore, inhibition of actin

polymerization significantly reversed the impaired degranulation in MYO1F- silenced cells, suggesting that MYO1F is important for cortical actin reorganization after IgE activation.

In macrophages, MYO1F, and the closely related MYO1E are required for phagocytosis of antibody-opsonized targets by macrophages. In the absence of these myosins, the organization of individual adhesions is compromised, leading to excessive actin polymerization, slower adhesion turnover and deficient cup closure during phagocytosis (18). Also, the M1-phenotype polarization of macrophages, which is mediated by integrin-αVβ3, relies on the presence of MYO1F (17), which collaborates with MYO1E for efficient LPS-induced spreading (58). In a zebrafish model, MYO1F appears to be crucial for maintaining the blastodisc morphology and the actin cortex thickness (59). Altogether, the role of MYO1F in these different models point to an involvement of this myosin in actin reorganization in agreement with our data in mast cells.

Although total calcium responses were not altered in MYO1F-silenced cells, calcium mobilization in the absence of extracellular calcium, which represent release from intracellular stores, was slightly but significantly reduced in the first few minutes of mobilization. Mitochondria contribute to the regulation of Ca2+ mobilization by coupling with the endoplasmic reticulum and maintaining Ca2+ oscillations (60). Moreover, mitochondrial structure is necessary for degranulation, as shown by the use of the antimicrobial agent triclosan (TCS), which disrupts mitochondrial nanostructure leading to a defective function that decreases mast cell degranulation capacity (61). Furthermore, it has been reported that mitochondria undergo fission and translocation to the cell membrane after mast cell activation and that this translocation is necessary for degranulation and TNF secretion (37). Interestingly, we observed a diminished mitochondria fission capacity after stimulation and defective translocation to the plasma membrane in MYO1F-knockdown cells, which could have contributed to the defective degranulation and TNF secretion. Additionally, blockade of F-actin polymerization/depolymerization has been reported to alter the mitochondrial network (62). Our results show that inhibitors of polymerization reverse significantly the defective degranulation in MYO1F-silenced cells, so we hypothesize that MYO1F downregulation may alter actin filament dynamics and subsequently alter mitochondrial organization. Reinforcing a role of MYO1F in mitochondrial network, a mutation in MYO1F (Gly134Ser) in thyroid cancer cells has been reported to confer an altered mitochondrial network and induce tumor proliferation. MYO1F G134S increased mitochondrial mass but did not impair mitochondrial membrane potential or dynamin-related protein 1 (DRP1) phosphorylation, a protein involved in mitochondrial fission (63, 64). This data is consistent with our results in MYO1F-deficient cells, which showed defective degranulation but a normal mitochondrial membrane potential.

Dynamin-related protein 1 (DRP-1) is essential for mitochondria fission process (43, 64). According to Ji et al., DRP1-dependent fission process can be explained in three steps: recruitment, maturation, and conversion (65). During the recruitment, DRP1 binds F-actin in the cytosol and translocates to the mitochondria. Actin-dependent localization of DRP-1 to (17)mitochondria requires a Myosin (66–68). Then, DRP1 is phosphorylated of Ser616 and this modification contributes to mitochondrial localization of DRP1 and promotes mitochondrial fission (41). Our results show that after IgE- and MRGPRX2- dependent mast

cell activation, the phosphorylation levels of DRP-1 are significantly reduced in MYO1F-silenced cells. However, ERK1/2 activity (involved in DRP-1 phosphorylation) (69) remained comparable in control and silenced cells. In contrast, MYO1F silencing reduced AKT phosphorylation. Consistent with our data, Myo1f has been reported to regulate AKT phosphorylation in macrophages (17). The way to do that could be related to actin dynamics where the role of a myosin stabilizing actin cytoskeleton could play a key role. In this context, it has been reported that AKT associates with the actin cytoskeleton, through the N-terminal PH domain of AKT (70). The same authors show that concomitant with association there is an increase in AKT phosphorylation and suggest that Cdc42 seems to facilitate AKT actin binding, possibly increasing AKT phosphorylation. Although AKT activity has been directly linked to DRP1 phosphorylation and mitochondrial fission in an Alzheimer's disease model (71) more experiments are needed to fully understand the AKT-DRP1 pathway. Altogether, our data points that MYO1F is crucial for AKT activation and DRP1 phosphorylation controlling mitochondrial fission. Further experiments will be needed to dissect this signaling.

MYO1F apart from the N-terminal motor domain (actin binding), light-chain binding IQ motifs (calmodulin binding) and a basic tail homology 1 (TH1) thought to interact with membranes has an additional proline-rich TH2 domain and a TH3 domain containing a single Src homology (SH3) domain (72). Recently, our group reported that the SH3 domain of MYO1F binds the adaptor protein 3BP2, which regulates both KIT migration and survival as well as FcεRI dependent degranulation (11, 13, 14). Our study links MYO1F to IgE and non-IgE receptor-induced signaling pathways and their function, and describes a role for this protein on on actin mesh dynamics. Since MRGPRX2 has emerged as an important receptor in mast cells contributing to innate and adaptive immunity, chronic allergic diseases and potentially neurogenic inflammation, pain and itch (73), our data may have wider implications in mast cell biology beyond allergic inflammation. In macrophages, MYO1F is specifically localized to the Fc-receptor adhesions and is required for efficient phagocytosis of antibody-opsonized targets (18). Interestingly, the adaptor protein 3BP2 is also required for optimal FcRγ- mediated phagocytosis and chemokine expression in macrophages (74) which points that both partners may play a role in cytoskeleton dynamics in macrophages and mast cells.

A better understanding of mediator-specific trafficking and its regulatory pathways by cytoskeleton-interacting motor proteins may bring us new information and hopefully therapeutic targets for the treatment of increasingly widespread mast-cell-related diseases.

Supplementary Material

Refer to Web version on PubMed Central for supplementary material.

ACKNOWLEDGEMENTS

We are indebted to the service of advanced optical and electron microscopy of the CCIT (University of Barcelona) and to the Cytomics core facility of the *Institut d'Investigacions Biomèdiques August Pi i Sunyer* (IDIBAPS) for their technical support. Graphical abstract was retrieved from https://app.biorender.com/biorender-templates.

This study has been funded by grants of the Spanish Ministry for Economy and Competitiveness/Spanish Ministry of Science Innovation and Universities and European Regional Development Fund/European Social Fund "Investing in your future": SAF2015-68124-R and RTI2018-096915-B100 and a grant issued by the *Instituto de Salud Carlos III* (ISCIII), co-funded by the *Fondo Europeo de Desarrollo Regional (*FEDER) for the Thematic Networks and Co-operative Research Centres: ARADyAL (RD16/0006/0007 and RD16/0006/0031). This work was supported in part by the Division of Intramural Research of the National Institutes of Health (NIH), National Institute of Allergy and Infectious Diseases (NIAID). AN-F was supported by a grant from Fundación Gangoiti Barrera.

BIBLIOGRAPHY

1. Wernersson S, and Pejler G. 2014. Mast cell secretory granules: armed for battle. Nat. Rev. Immunol. 14: 478–494. [PubMed: 24903914]
2. Galli SJ, Grimbaldeston M, and Tsai M. 2008. Immunomodulatory mast cells: negative, as well as positive, regulators of immunity. Nat. Rev. Immunol. 8: 478–486. [PubMed: 18483499]
3. Yu Y, Blokhuis BR, Garssen J, and Redegeld FA. 2016. Non-IgE mediated mast cell activation. Eur. J. Pharmacol. 778: 33–43. [PubMed: 26164792]
4. Marshall JS 2004. Mast-cell responses to pathogens. Nat. Rev. Immunol. 4: 787–799. [PubMed: 15459670]
5. Fujisawa D, Kashiwakura J, Kita H, Kikukawa Y, Fujitani Y, Sasaki-Sakamoto T, Kuroda K, Nunomura S, Hayama K, Terui T, Ra C, and Okayama Y. 2014. Expression of Mas-related gene X2 on mast cells is upregulated in the skin of patients with severe chronic urticaria. J. Allergy Clin. Immunol. 134: 622–633.e9. [PubMed: 24954276]
6. McNeil BD, Pundir P, Meeker S, Han L, Undem BJ, Kulka M, and Dong X. 2015. Identification of a mast-cell-specific receptor crucial for pseudo-allergic drug reactions. Nature 519: 237–241. [PubMed: 25517090]
7. Navinés-Ferrer A, Serrano-Candelas E, Lafuente A, Muñoz-Cano R, Martín M, and Gastaminza G. 2018. MRGPRX2-mediated mast cell response to drugs used in perioperative procedures and anaesthesia. Sci. Rep. 8: 11628. [PubMed: 30072729]
8. Dráber P, Sulimenko V, and Dráberová E. 2012. Cytoskeleton in Mast Cell Signaling. Front. Immunol. 3. [PubMed: 22566889]
9. Nishida K, Yamasaki S, Ito Y, Kabu K, Hattori K, Tezuka T, Nishizumi H, Kitamura D, Goitsuka R, Geha RS, Yamamoto T, Yagi T, and Hirano T. 2005. FcεRI-mediated mast cell degranulation requires calcium-independent microtubule-dependent translocation of granules to the plasma membrane. J. Cell Biol. 170: 115–126. [PubMed: 15998803]
10. Dráber P, and Dráber P. 2015. Membrane-Cytoskeleton Dynamics in the Course of Mast Cell Activation. In Methods in Molecular Biology 219–237.
11. Navinés-Ferrer A, Ainsua-Enrich E, Serrano-Candelas E, Sayós J, and Martin M. 2019. Myo1f, an Unconventional Long-Tailed Myosin, Is a New Partner for the Adaptor 3BP2 Involved in Mast Cell Migration. Front. Immunol. 10. [PubMed: 30723470]
12. Navinés-Ferrer A, and Martín M. 2020. Long-Tailed Unconventional Class I Myosins in Health and Disease. Int. J. Mol. Sci. 21: 2555.
13. Ainsua-Enrich E, Serrano-Candelas E, Álvarez-Errico D, Picado C, Sayós J, Rivera J, and Martín M. 2015. The Adaptor 3BP2 Is Required for KIT Receptor Expression and Human Mast Cell Survival. J. Immunol. 194: 4309–4318. [PubMed: 25810396]
14. Ainsua-Enrich E, Álvarez-Errico D, Gilfillan AM, Picado C, Sayós J, Rivera J, and Martín M. 2012. The Adaptor 3BP2 Is Required for Early and Late Events in FcεRI Signaling in Human Mast Cells. J. Immunol. 189: 2727–2734. [PubMed: 22896635]
15. Kim SV, Mehal WZ, Dong X, Heinrich V, Pypaert M, Mellman I, Dembo M, Mooseker MS, Wu D, and Flavell RA. 2006. Modulation of Cell Adhesion and Motility in the Immune System by Myo1f. Science (80-.). 314: 136–139.
16. Salvermoser M, Pick R, Weckbach LTT, Zehrer A, Löhr P, Drechsler M, Sperandio M, Soehnlein O, and Walzog B. 2018. Myosin 1f is specifically required for neutrophil migration in 3D environments during acute inflammation. Blood 131: 1887–1898. [PubMed: 29487067]

17. Piedra-Quintero ZL, Serrano C, Villegas-Sepúlveda N, Maravillas-Montero JL, Romero-Ramírez S, Shibayama M, Medina-Contreras O, Nava P, and Santos-Argumedo L. 2019. Myosin 1F Regulates M1-Polarization by Stimulating Intercellular Adhesion in Macrophages. Front. Immunol. 9. [PubMed: 30809220]

18. Barger SR, Reilly NS, Shutova MS, Li Q, Maiuri P, Heddleston JM, Mooseker MS, Flavell RA, Svitkina T, Oakes PW, Krendel M, and Gauthier NC. 2019. Membrane-cytoskeletal crosstalk mediated by myosin-I regulates adhesion turnover during phagocytosis. Nat. Commun. 10: 1249. [PubMed: 30890704]

19. Kirshenbaum AS, Akin C, Wu Y, Rottem M, Goff JP, Beaven MA, Rao VK, and Metcalfe DD. 2003. Characterization of novel stem cell factor responsive human mast cell lines LAD 1 and 2 established from a patient with mast cell sarcoma/leukemia; activation following aggregation of FcεRI or FcγRI. Leuk. Res. 27: 677–682. [PubMed: 12801524]

20. Rådinger M, Jensen BM, Kuehn HS, Kirshenbaum A, and Gilfillan AM. 2010. Generation, Isolation, and Maintenance of Human Mast Cells and Mast Cell Lines Derived from Peripheral Blood or Cord Blood. In Current Protocols in Immunology John Wiley & Sons, Inc., Hoboken, NJ, USA.

21. Wiederschain D, Susan W, Chen L, Loo A, Yang G, Huang A, Chen Y, Caponigro G, Yao Y, Lengauer C, Sellers WR, and Benson JD. 2009. Single-vector inducible lentiviral RNAi system for oncology target validation. Cell Cycle 8: 498–504. [PubMed: 19177017]

22. Tůmová M, Koffer A, Šimíček M, Dráberová L, and Dráber P. 2010. The transmembrane adaptor protein NTAL signals to mast cell cytoskeleton via the small GTPase Rho. Eur. J. Immunol. 40: 3235–3245. [PubMed: 21061444]

23. Subramanian H, Gupta K, and Ali H. 2016. Roles of Mas-related G protein–coupled receptor X2 on mast cell–mediated host defense, pseudoallergic drug reactions, and chronic inflammatory diseases. J. Allergy Clin. Immunol. 138: 700–710. [PubMed: 27448446]

24. Moon TC, Befus AD, and Kulka M. 2014. Mast Cell Mediators: Their Differential Release and the Secretory Pathways Involved. Front. Immunol. 5. [PubMed: 24478774]

25. Taracanova A, Alevizos M, Karagkouni A, Weng Z, Norwitz E, Conti P, Leeman SE, and Theoharides TC. 2017. SP and IL-33 together markedly enhance TNF synthesis and secretion from human mast cells mediated by the interaction of their receptors. Proc. Natl. Acad. Sci. 114: E4002–E4009. [PubMed: 28461492]

26. Gordon JR, and Galli SJ. 1990. Mast cells as a source of both preformed and immunologically inducible TNF-α/cachectin. Nature 346: 274–276. [PubMed: 2374592]

27. Spiering D, and Hodgson L. 2011. Dynamics of the Rho-family small GTPases in actin regulation and motility. Cell Adh. Migr. 5: 170–180. [PubMed: 21178402]

28. Hong-Geller E, and Cerione RA. 2000. Cdc42 and Rac Stimulate Exocytosis of Secretory Granules by Activating the Ip3/Calcium Pathway in Rbl-2h3 Mast Cells. J. Cell Biol. 148: 481–494. [PubMed: 10662774]

29. Malacombe M, Ceridono M, Calco V, Chasserot-Golaz S, McPherson PS, Bader M-F, and Gasman S. 2006. Intersectin-1L nucleotide exchange factor regulates secretory granule exocytosis by activating Cdc42. EMBO J. 25: 3494–3503. [PubMed: 16874303]

30. Zhang X, Bi E, Novick P, Du L, Kozminski KG, Lipschutz JH, and Guo W. 2001. Cdc42 Interacts with the Exocyst and Regulates Polarized Secretion. J. Biol. Chem. 276: 46745–46750. [PubMed: 11595741]

31. Balseiro-Gomez S, Flores JA, Acosta J, Ramirez-Ponce MP, and Ales E. 2016. Transient fusion ensures granule replenishment to maintain repeated release after IgE-mediated mast cell degranulation. J. Cell Sci. 129: 3989–4000. [PubMed: 27624612]

32. Frigeri L, and Apgar JR. 1999. The role of actin microfilaments in the down-regulation of the degranulation response in RBL-2H3 mast cells. J. Immunol. 162: 2243–50. [PubMed: 9973500]

33. Pfeiffer JR, Seagrave JC, Davis BH, Deanin GG, and Oliver JM. 1985. Membrane and cytoskeletal changes associated with IgE-mediated serotonin release from rat basophilic leukemia cells. J. Cell Biol. 101: 2145–2155. [PubMed: 2933414]

34. Colin-York H, Li D, Korobchevskaya K, Chang VT, Betzig E, Eggeling C, and Fritzsche M. 2019. Cytoskeletal actin patterns shape mast cell activation. Commun. Biol. 2: 93. [PubMed: 30854485]

35. Cohen R, Corwith K, Holowka D, and Baird B. 2012. Spatiotemporal resolution of mast cell granule exocytosis reveals correlation with Ca 2+ wave initiation. J. Cell Sci. 125: 2986–2994. [PubMed: 22393234]
36. Takekawa M, Furuno T, Hirashima N, and Nakanishi M. 2012. Mitochondria Take Up Ca2+ in Two Steps Dependently on Store-Operated Ca2+ Entry in Mast Cells. Biol. Pharm. Bull. 35: 1354–1360. [PubMed: 22863937]
37. Zhang B, Alysandratos K-D, Angelidou A, Asadi S, Sismanopoulos N, Delivanis D-A, Weng Z, Miniati A, Vasiadi M, Katsarou-Katsari A, Miao B, Leeman SE, Kalogeromitros D, and Theoharides TC. 2011. Human mast cell degranulation and preformed TNF secretion require mitochondrial translocation to exocytosis sites: Relevance to atopic dermatitis. J. Allergy Clin. Immunol. 127: 1522–1531.e8. [PubMed: 21453958]
38. Youle RJ, and van der Bliek AM. 2012. Mitochondrial fission, fusion, and stress. Science 337: 1062–5. [PubMed: 22936770]
39. Quintana A, and Hoth M. 2012. Mitochondrial dynamics and their impact on T cell function. Cell Calcium 52: 57–63. [PubMed: 22425631]
40. Serasinghe MN, Wieder SY, Renault TT, Elkholi R, Asciolla JJ, Yao JL, Jabado O, Hoehn K, Kageyama Y, Sesaki H, and Chipuk JE. 2015. Mitochondrial Division Is Requisite to RAS-Induced Transformation and Targeted by Oncogenic MAPK Pathway Inhibitors. Mol. Cell 57: 521–536. [PubMed: 25658204]
41. Otera H, Ishihara N, and Mihara K. 2013. New insights into the function and regulation of mitochondrial fission. Biochim. Biophys. Acta - Mol. Cell Res. 1833: 1256–1268.
42. Zhang B, Weng Z, Sismanopoulos N, Asadi S, Therianou A, Alysandratos K-D, Angelidou A, Shirihai O, and Theoharides TC. 2012. Mitochondria Distinguish Granule-Stored from de novo Synthesized Tumor Necrosis Factor Secretion in Human Mast Cells. Int. Arch. Allergy Immunol. 159: 23–32. [PubMed: 22555146]
43. Frank S, Gaume B, Bergmann-Leitner ES, Leitner WW, Robert EG, Catez F, Smith CL, and Youle RJ. 2001. The Role of Dynamin-Related Protein 1, a Mediator of Mitochondrial Fission, in Apoptosis. Dev. Cell 1: 515–525. [PubMed: 11703942]
44. Otera H, and Mihara K. 2011. Discovery of the membrane receptor for mitochondrial fission GTPase Drp1. Small GTPases 2: 167–172. [PubMed: 21776419]
45. Taguchi N, Ishihara N, Jofuku A, Oka T, and Mihara K. 2007. Mitotic Phosphorylation of Dynamin-related GTPase Drp1 Participates in Mitochondrial Fission. J. Biol. Chem. 282: 11521–11529. [PubMed: 17301055]
46. Qi X, Disatnik M-H, Shen N, Sobel RA, and Mochly-Rosen D. 2011. Aberrant mitochondrial fission in neurons induced by protein kinase Cδ under oxidative stress conditions in vivo. Mol. Biol. Cell 22: 256–265. [PubMed: 21119009]
47. Nagdas S, and Kashatus DF. 2017. The Interplay between Oncogenic Signaling Networks and Mitochondrial Dynamics. Antioxidants 6: 33.
48. Klein O, and Sagi-Eisenberg R. 2019. Anaphylactic Degranulation of Mast Cells: Focus on Compound Exocytosis. J. Immunol. Res. 2019: 1–12.
49. Gaudenzio N, Sibilano R, Marichal T, Starkl P, Reber LL, Cenac N, McNeil BD, Dong X, Hernandez JD, Sagi-Eisenberg R, Hammel I, Roers A, Valitutti S, Tsai M, Espinosa E, and Galli SJ. 2016. Different activation signals induce distinct mast cell degranulation strategies. J. Clin. Invest. 126: 3981–3998. [PubMed: 27643442]
50. Matsuoka T 2000. Prostaglandin D2 as a Mediator of Allergic Asthma. Science (80-.). 287: 2013–2017.
51. Rius M, Hummel-Eisenbeiss J, and Keppler D. 2008. ATP-Dependent Transport of Leukotrienes B 4 and C 4 by the Multidrug Resistance Protein ABCC4 (MRP4). J. Pharmacol. Exp. Ther. 324: 86–94. [PubMed: 17959747]
52. Adachi H, Suzuki T, Abe M, Asano N, Mizutamari H, Tanemoto M, Nishio T, Onogawa T, Toyohara T, Kasai S, Satoh F, Suzuki M, Tokui T, Unno M, Shimosegawa T, Matsuno S, Ito S, and Abe T. 2003. Molecular characterization of human and rat organic anion transporter OATP-D. Am. J. Physiol. Physiol. 285: 54–56.

53. Olszewski MB, Groot AJ, Dastych J, and Knol EF. 2007. TNF Trafficking to Human Mast Cell Granules: Mature Chain-Dependent Endocytosis. J. Immunol. 178: 5701–5709. [PubMed: 17442953]
54. Ridley AJ 2006. Rho GTPases and actin dynamics in membrane protrusions and vesicle trafficking. Trends Cell Biol. 16: 522–529. [PubMed: 16949823]
55. Pivniouk VI 2003. Impaired signaling via the high-affinity IgE receptor in Wiskott-Aldrich syndrome protein-deficient mast cells. Int. Immunol. 15: 1431–1440. [PubMed: 14645152]
56. Brzeska H, Bagnoli M, Korn ED, and Titus MA. 2020. Dictyostelium myosin 1F and myosin 1E inhibit actin waves in a lipid-binding-dependent and motor-independent manner. Cytoskeleton cm.21627.
57. Lin J-L, Chen C-G, Shen Z-Z, Piao Z-X, Li W-Q, Liu L, Xu L-Y, and Li E-M. 2014. Actin cytoskeleton reorganization correlates with polarization of secretory vesicle and cell morphology in the degranulation of mast cell subtypes in human colon tissues. Acta Histochem. 116: 407–414. [PubMed: 24161690]
58. Wenzel J, Ouderkirk JL, Krendel M, and Lang R. 2015. Class I myosin Myo1e regulates TLR4-triggered macrophage spreading, chemokine release, and antigen presentation via MHC class II. Eur. J. Immunol. 45: 225–237. [PubMed: 25263281]
59. Gupta P, Martin R, Knölker H-J, Nihalani D, and Kumar Sinha D. 2017. Myosin-1 inhibition by PClP affects membrane shape, cortical actin distribution and lipid droplet dynamics in early Zebrafish embryos. PLoS One 12: e0180301. [PubMed: 28678859]
60. Holowka D, Wilkes M, Stefan C, and Baird B. 2016. Roles for Ca2+ mobilization and its regulation in mast cell functions: recent progress. Biochem. Soc. Trans. 44: 505–509. [PubMed: 27068962]
61. Weatherly LM, Nelson AJ, Shim J, Riitano AM, Gerson ED, Hart AJ, de Juan-Sanz J, Ryan TA, Sher R, Hess ST, and Gosse JA. 2018. Antimicrobial agent triclosan disrupts mitochondrial structure, revealed by super-resolution microscopy, and inhibits mast cell signaling via calcium modulation. Toxicol. Appl. Pharmacol. 349: 39–54. [PubMed: 29630968]
62. Li S, Xu S, Roelofs BA, Boyman L, Lederer WJ, Sesaki H, and Karbowski M. 2015. Transient assembly of F-actin on the outer mitochondrial membrane contributes to mitochondrial fission. J. Cell Biol. 208: 109–123. [PubMed: 25547155]
63. Diquigiovanni C, Bergamini C, Evangelisti C, Isidori F, Vettori A, Tiso N, Argenton F, Costanzini A, Iommarini L, Anbunathan H, Pagotto U, Repaci A, Babbi G, Casadio R, Lenaz G, Rhoden KJ, Porcelli AM, Fato R, Bowcock A, Seri M, Romeo G, and Bonora E. 2018. Mutant MYO1F alters the mitochondrial network and induces tumor proliferation in thyroid cancer. Int. J. Cancer 143: 1706–1719. [PubMed: 29672841]
64. Fonseca TB, Sánchez-Guerrero Á, Milosevic I, and Raimundo N. 2019. Mitochondrial fission requires DRP1 but not dynamins. Nature 570: E34–E42. [PubMed: 31217603]
65. Ji W, Hatch AL, Merrill RA, Strack S, and Higgs HN. 2015. Actin filaments target the oligomeric maturation of the dynamin GTPase Drp1 to mitochondrial fission sites. Elife 4.
66. DuBoff B, Götz J, and Feany MB. 2012. Tau Promotes Neurodegeneration via DRP1 Mislocalization In Vivo. Neuron 75: 618–632. [PubMed: 22920254]
67. Hatch AL, Gurel PS, and Higgs HN. 2014. Novel roles for actin in mitochondrial fission. J. Cell Sci. 127: 4549–4560. [PubMed: 25217628]
68. De Vos KJ, Allan VJ, Grierson AJ, and Sheetz MP. 2005. Mitochondrial Function and Actin Regulate Dynamin-Related Protein 1-Dependent Mitochondrial Fission. Curr. Biol. 15: 678–683. [PubMed: 15823542]
69. Prieto J, León M, Ponsoda X, Sendra R, Bort R, Ferrer-Lorente R, Raya A, López-García C, and Torres J. 2016. Early ERK1/2 activation promotes DRP1-dependent mitochondrial fission necessary for cell reprogramming. Nat. Commun. 7: 11124. [PubMed: 27030341]
70. Cenni V, Sirri A, Riccio M, Lattanzi G, Santi S, De Pol A, Maraldi NM, and Marmiroli S. 2003. Targeting of the Akt/PKB kinase to the actin skeleton. Cell. Mol. Life Sci..
71. Kim DI, Lee KH, Gabr AA, Choi GE, Kim JS, Ko SH, and Han HJ. 2016. Aβ-Induced Drp1 phosphorylation through Akt activation promotes excessive mitochondrial fission leading to neuronal apoptosis. Biochim. Biophys. Acta - Mol. Cell Res..

72. Krendel M, and Mooseker MS. 2005. Myosins: Tails (and Heads) of Functional Diversity. Physiology 20: 239–251. [PubMed: 16024512]

73. Olivera A, Beaven MA, and Metcalfe DD. 2018. Mast cells signal their importance in health and disease. J. Allergy Clin. Immunol. 142: 381–393. [PubMed: 29454835]

74. Chihara K, Kato Y, Yoshiki H, Takeuchi K, Fujieda S, and Sada K. 2017. Syk-dependent tyrosine phosphorylation of 3BP2 is required for optimal FcRγ-mediated phagocytosis and chemokine expression in U937 cells. Sci. Rep. 7: 11480. [PubMed: 28904407]

Key points:

- Myo1f regulates IgE and MRGPRX2-dependent mast cell degranulation
- Myo1f regulates actin cytoskeleton dynamics and distribution of secretory granules
- Myo1f is required for mitochondria fission and location in activated mast cells

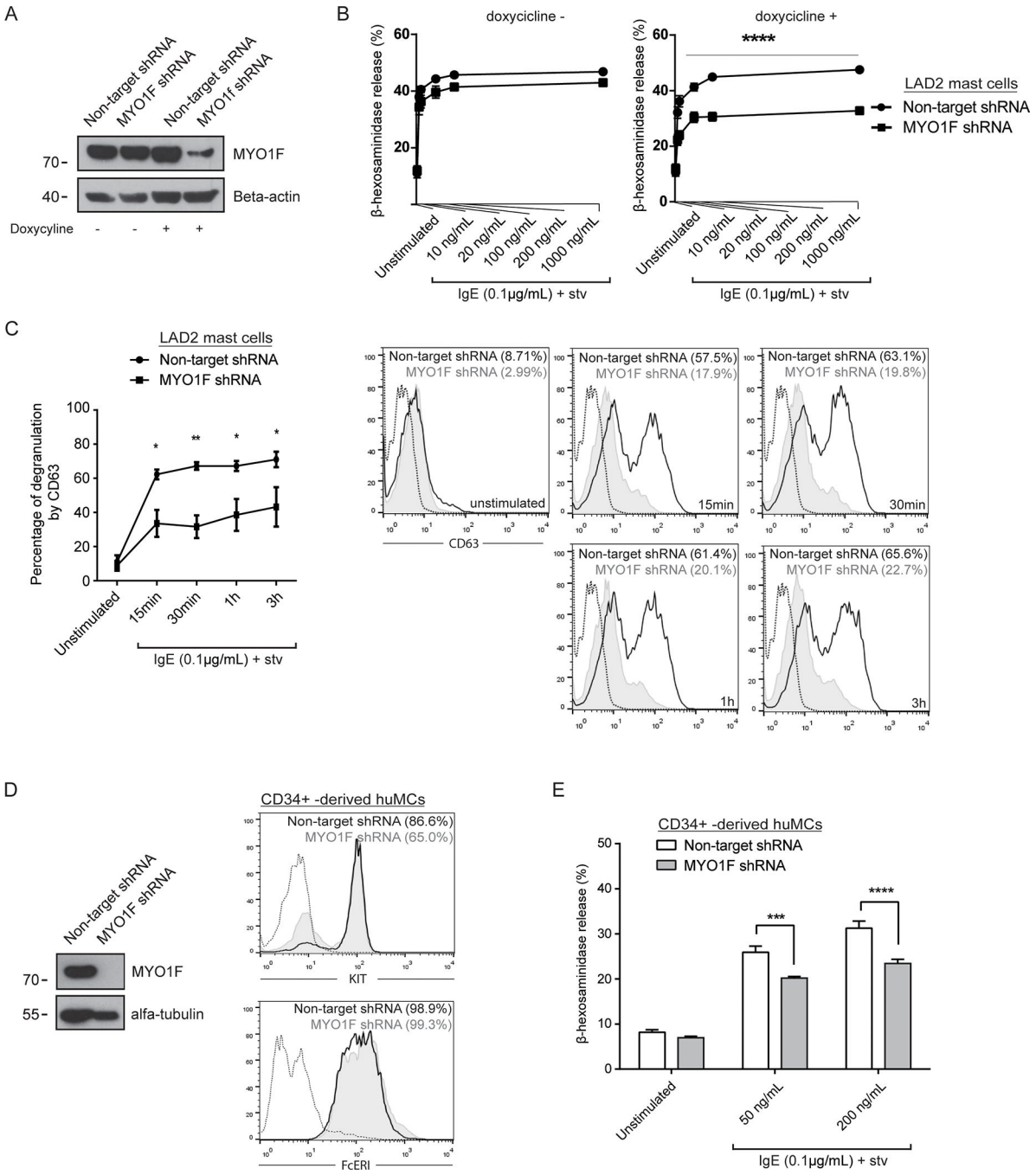

Figure 1. MYO1F-knockdown reduces IgE-mediated degranulation.

(A) Doxycycline was used in the culture media to induce MYO1F silencing and doxycycline-untreated cells were used as a control. Knockdown was confirmed by western blot. (B) Control (non-target shRNA) and MYO1F-deficient (MYO1F-shRNA) pre-bound with IgEB LAD2 mast cells were stimulated with different doses of streptavidin for 30 minutes to induce IgE crosslinking. β-hexosaminidase activity in the supernatant was measured as a percentage of total activity. (C) Non-target and MYO1F- shRNA pre-bound with IgEB LAD2 mast cells were stimulated at different times with streptavidin (200 ng/mL)

to induce IgE crosslinking. The percentage of positive cells was determined in relation to the isotype control. Non-target shRNA is represented by an empty black curve and MYO1F-shRNA is represented by a grey filled curve. (D) CD34+ - derived huMCs were transduced with MYO1F shRNA or non-target shRNA and the silencing was confirmed by western blot. Expression of KIT and FcεRI was determined by flow cytometry. Non-target shRNA is represented by an empty black curve and MYO1F-shRNA is represented by a grey filled curve. (E) Control (non-target shRNA) and MYO1F-deficient (MYO1F-shRNA) huMCs were stimulated with different doses of streptavidin for 30 minutes to induce IgE crosslinking. β- hexosaminidase activity in the supernatant was measured as a percentage of total activity. One-way ANOVA test was used for the statistical analysis (*$p<0.05$, **$p<0.01$, ***$p<0.001$, ****$p<0.0001$).

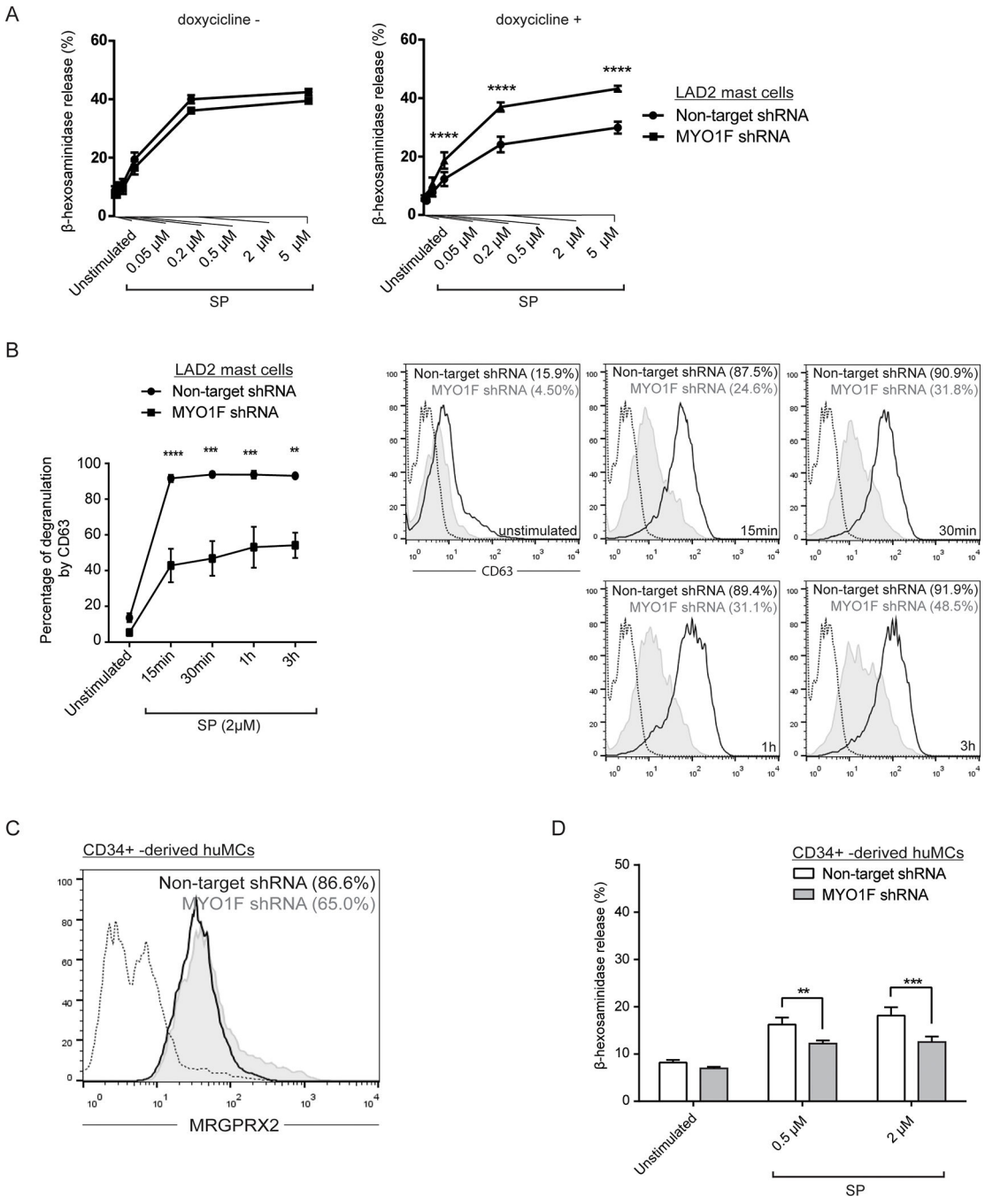

Figure 2. MYO1F-knockdown reduces MRGPRX2-mediated degranulation.

(A) Doxycycline was used in the culture media to induce MYO1F silencing and doxycycline-untreated cells were used as a control. Control (non-target shRNA) and MYO1F-deficient (MYO1F-shRNA) LAD2 mast cells were stimulated with different doses of substance P for 30 min. β-hexosaminidase activity in the supernatant was measured as a percentage of total activity. (B) Non-target and MYO1F-shRNA LAD2 mast cells were stimulated at different times with substance P (2 μM). The percentage of positive cells was determined in relation to the isotype control. Non-target shRNA is represented by an empty

black curve and MYO1F-shRNA is represented by a grey filled curve. (C) Expression of MRGPRX2 receptor in CD34+ -derived huMCs transduced with MYO1F shRNA or non-target shRNA was determined by flow cytometry. Non-target shRNA is represented by an empty black curve and MYO1F-shRNA is represented by a grey filled curve. (D) Control (non-target shRNA) and MYO1F-deficient (MYO1F-shRNA) huMCs were stimulated with different doses of substance P for 30 minutes. β-hexosaminidase activity in the supernatant was measured as a percentage of total activity. One-way ANOVA test was used for the statistical analysis (**$p<0.01$, ***$p<0.001$, ****$p<0.0001$).

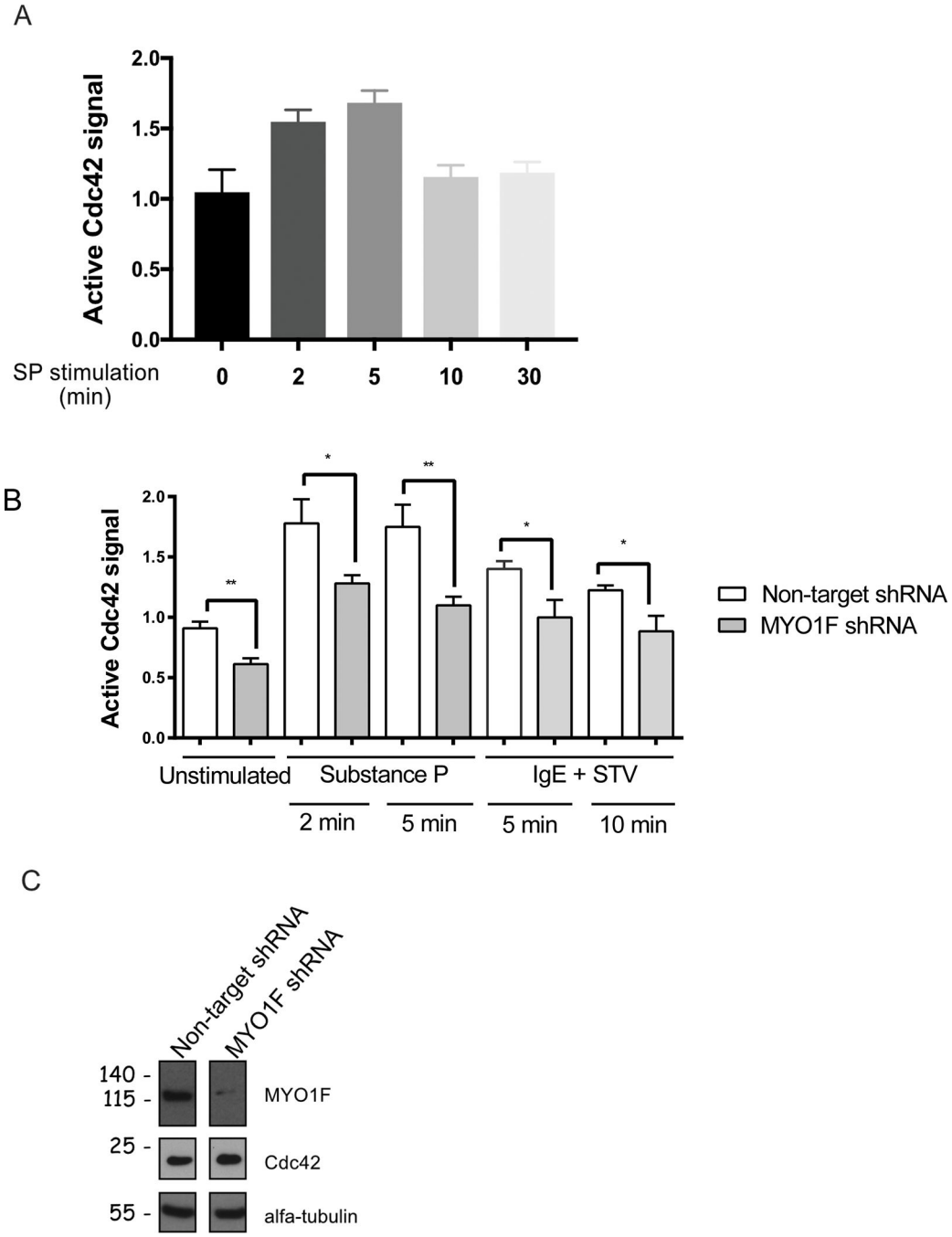

Figure 3. MYO1F Is Required for Cdc42 Activation in Mast Cells.

G-Lisa quantification of GTP-bound (active) small GTPases Cdc42 was performed after substance P activation for several time points in LAD2 cells (A). IgE^B + streptavidin (400 ng/mL) or substance P (2 μM) cell activation for the indicated times in Control (Non-target shRNA) and MYO1F-knockdown (MYO1F-shRNA) LAD2 mast cells (B). Western Blot showing Cdc42 GTPase levels in NT and MYO1F-silenced cells (C). The student-t test was used for the statistical analysis (*$p<0.05$, **$p < 0.01$). Data are the mean of three independent experiments.

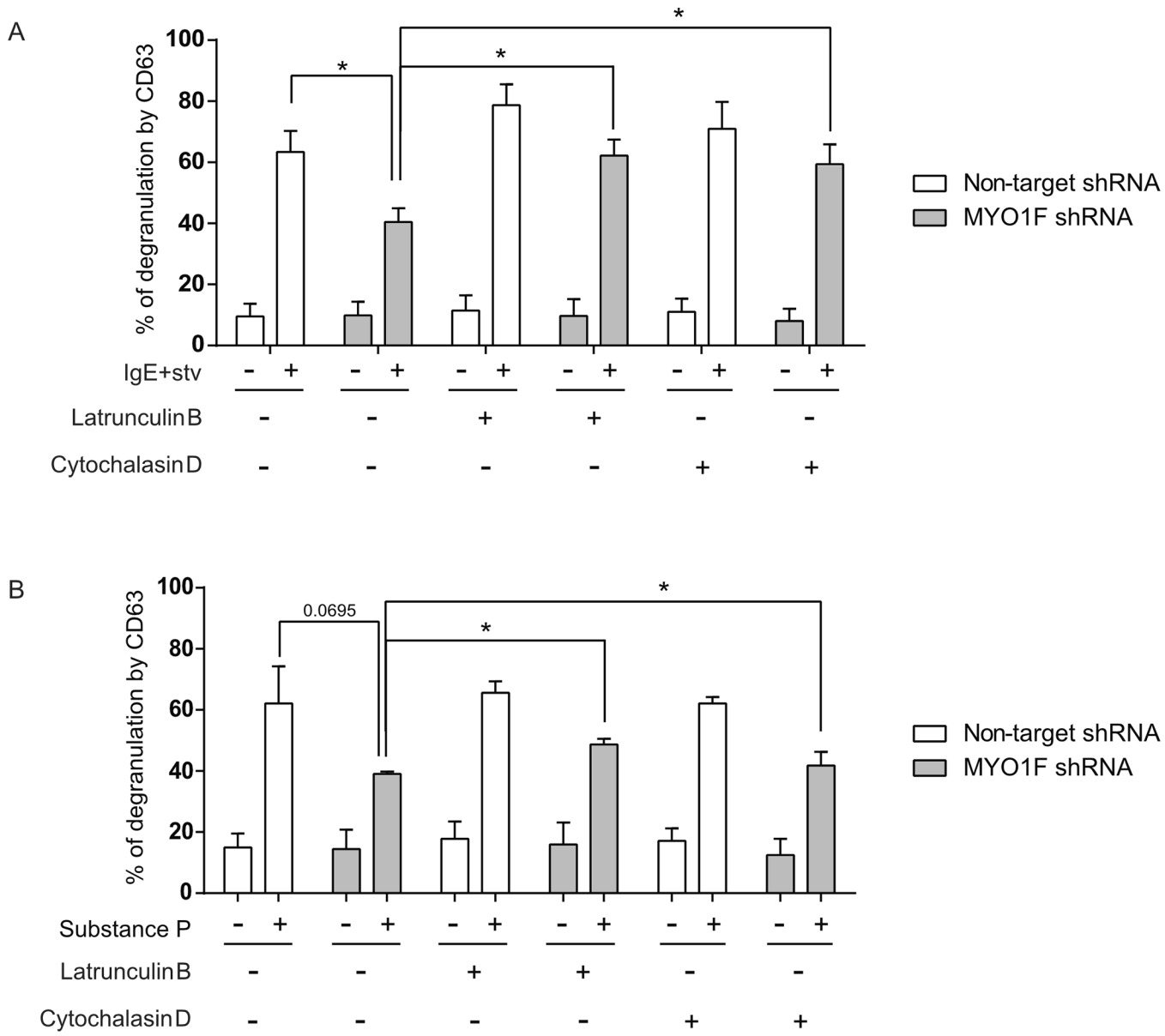

Figure 4. Inhibition of actin polymerization recovers the degranulation ability of MYO1F-silenced cells.

Control (non-target shRNA) and MYO1F-knockdown (MYO1F shRNA) LAD2 mast cells in the presence of doxycycline (0.5 μg/mL) were treated for 20 minutes with Latrunculin B or Cytochalasin D before stimulating them with (A) IgEB + streptavidin (200 ng/mL) or (B) Substance P (2 μM) for 30 minutes. The percentage of degranulation was determined by flow cytometry using CD63 staining. One-way ANOVA test was used for the statistical analysis (*$p<0.05$).

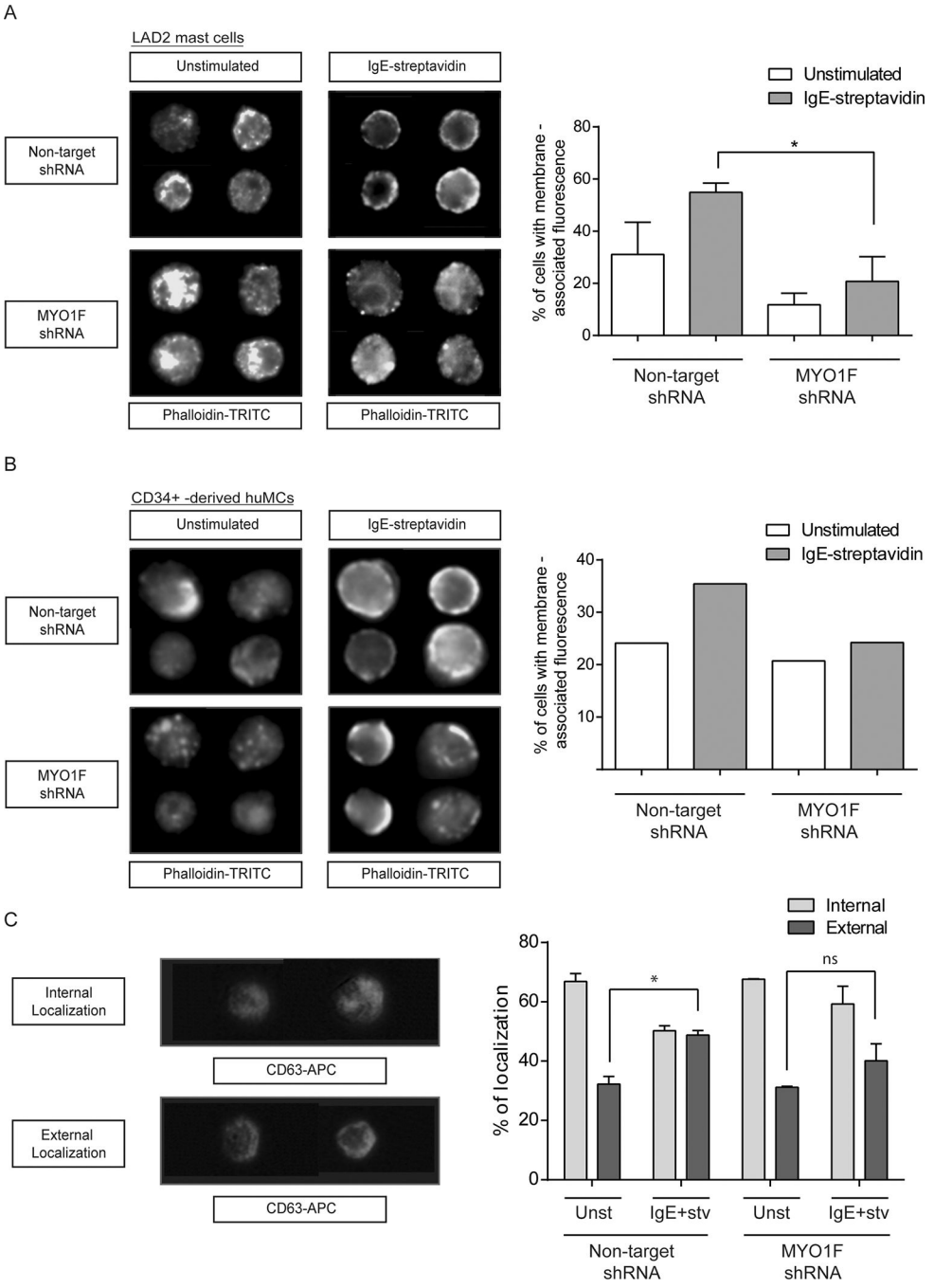

Figure 5. The downregulation of MYO1F alters the cortical actin ring after FcεRI activation and reduces granule localization close to the cell membrane after IgE- dependent activation.

(A) Control (non-target shRNA) and MYO1F-knockdown (MYO1F shRNA) LAD2 mast cells in the presence of doxycycline (0.5 μg/mL) with or without stimulation with IgEB+ streptavidin (200 ng/mL) for 15 minutes were fixed and analyzed in the imaging flow cytometer. Each group was divided into two sub-groups, one with low translocation of actin to the cell membrane and another with high translocation and a clearly visible cortical actin ring (actin is shown in yellow). The percentage of cells with a visible actin ring is

represented and compared with the other groups. (B) Control (non-target shRNA) and MYO1F-knockdown (MYO1F shRNA)
CD34+ huMCs stimulated or not with IgEB + streptavidin (200 ng/mL) were fixed and analyzed in the imaging flow cytometer as described in A. (C) Control (non-target shRNA) and MYO1F-knockdown (MYO1F shRNA) LAD2 mast cells in the presence of doxycycline (0.5 μg/mL) stimulated or not with IgEB + streptavidin (200 ng/mL) were fixed and analyzed in the imaging flow cytometer. They were divided into two sub-groups, one in which CD63 expression was close to the center of the cell (internal) and the other in which CD63 expression was at the periphery (external). The percentages are represented and compared between groups. One-way ANOVA test was used for the statistical analysis (ns= not significant, *$p<0.05$).

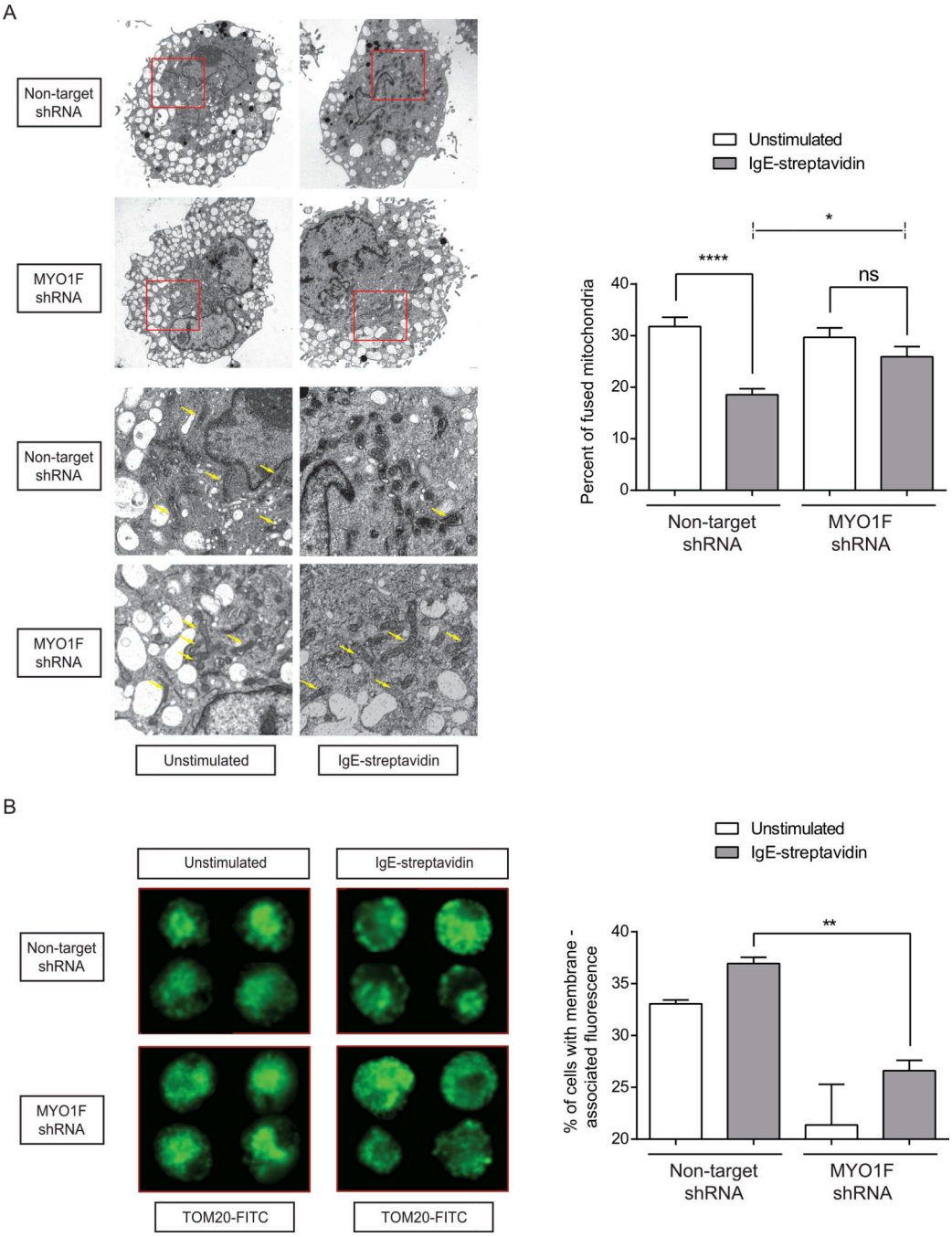

Figure 6. Mitochondria do not translocate to the cell membrane and present fewer fission events in MYO1F-silenced cells after FceRI activation.

(A) Non-target shRNA and MYO1F shRNA LAD2 mast cells in the presence of doxycycline (0.5 μg/mL) were stimulated with IgEB + streptavidin (200 ng/mL) for 30 minutes and fixed and prepared for electronic microscopy. Total mitochondria were counted using ImageJ software and the percentage of elongated mitochondria (elongated mitochondria are indicated by yellow arrows in the magnified image) was compared between groups. (B) Non-target shRNA and MYO1F shRNA LAD2 mast cells unstimulated or activated with IgEB + streptavidin (200 ng/mL) for 15 minutes were fixed and analyzed in the imaging

flow cytometer. Each group was divided into two sub-groups, one with low translocation of mitochondria to the cell membrane and another with high translocation (mitochondria are shown in green). The percentage of cells with high translocation is represented and compared with the other groups. One-way ANOVA was used for the statistical analysis (ns= not significant, *p<0.05, **p<0.01, ****p<0.0001).

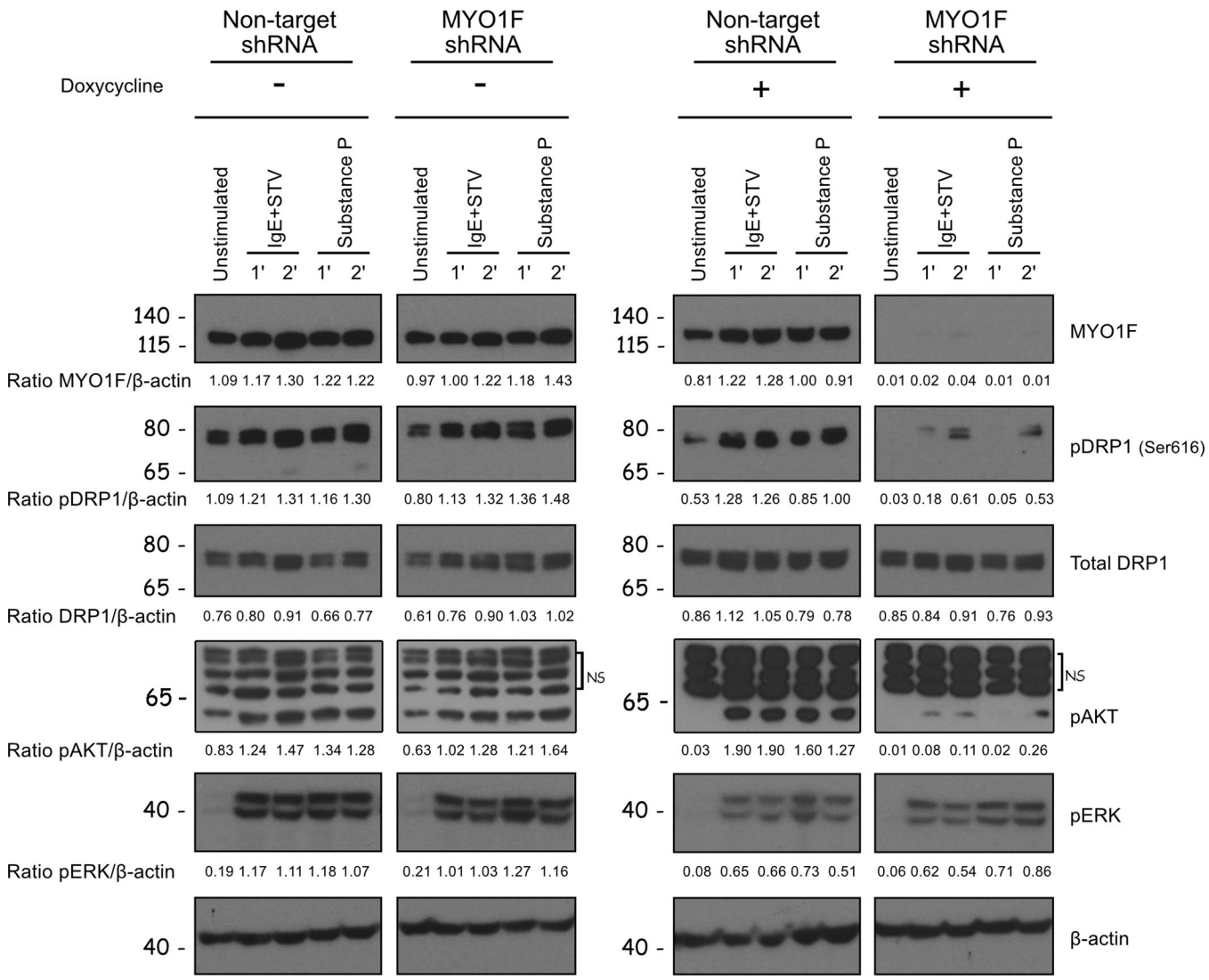

Figure 7. MYO1F knockdown does affect DRP1 phosphorylation on Ser 616 after FcεRI and MRGPRX2 activation.

Control (Non-target shRNA) and MYO1F-knockdown (MYO1F-shRNA) LAD2 mast cells in the presence or not of Doxycycline (0.5 μg/mL) were sensitized with IgE^B or left untreated. Next day cells were challenged with streptavidin (400 ng/mL). On the other hand, cells were treated with substance P (2 μM) for the indicated times. Western blots probed with the following Abs: anti-Myo1f, anti-pDRP1 (Ser 616), anti-DRP1, anti-pAKT(Ser 473), anti-pERK and anti-beta-actin (used as loading control). Band intensity for each blot was quantified by densitometry. NS: non-specific bands.